

# Inhibition effect of famotidine towards the corrosion of C-steel in sulphuric acid Solution

S. Abd El Wanees<sup>1,3,\*</sup>, M. A. Elmorsi<sup>2</sup>, T.A. Fayed<sup>2</sup>, A.S. Fouda<sup>4</sup> and S.S. Elyan<sup>5</sup>

1. Chemistry Department, Faculty of Science, Zagazig University, Zagazig, Egypt.
2. Chemistry Department, Faculty of Science, Tanta University, Tanta, Egypt.
3. Chemistry Department, Faculty of Science, Tabuk University, Tabuk, Saudi Arabia.
4. Chemistry Department, Faculty of Science, Mansoura University, Mansoura, Egypt.
5. Chemistry Department, Faculty of Pharmacy, Badr University In Cairo, Badr, Egypt.

## Abstract

The inhibition effect of famotidine drug towards the corrosion of C-steel in 0.5M H<sub>2</sub>SO<sub>4</sub> was studied using weight loss, gasometry, potentiodynamic polarization and electrochemical frequency modulation (EFM) techniques, as well as, surface examination by SEM. The inhibition mechanism of FA is based on the adsorption process forming a film barrier layer protect the steel from acid attack. The adsorption is found to obey Frundlich model. The inhibition efficiency increased by increasing inhibitor concentration and decreased with temperature. Some thermodynamic parameters for adsorption process are deduced and discussed.

**Keywords:** C-steel, famotidine, Adsorption, Corrosion.

## 1. Introduction

The corrosion inhibition of C-steel took great efforts of scientists and researchers especially in acid solution. The practical importance of this aspect is found in many fields, among of which, the acid pickling of iron and steel, electro-polishing, chemical cleaning and processing, metallic ores production, oil recovery and petrochemical industries. Hydrochloric acid is consider as an important mineral acid used in previous fields (Bentiss *et al.* 2001), (Chetouani *et al.* 2003), (Ashassi-Sorkhabi *et al.* 2004), (Ashassi-Sorkhabi *et al.* 2005), (Daoud *et al.* 2015),. The effective inhibitor is generally required in these processes to control the metal distortion process and acid consumption. Actually, the most effective acid corrosion inhibitors are bulky organic molecules that carry heteroatoms (N, S and O atoms) and give higher inhibition efficiency (El Azzouzi *et al.* 2016), (Evelin *et al.* 2016), (Abd El-Lateef *et al.* 2016), (Kowsari *et al.* 2016), (Pourghasemi *et al.* 2016).

Among the development of effective green inhibitors with high protection efficiency and environmentally save are the natural and nontoxic drugs that are used to resist the corrosion of steel in many aqueous solutions (Sangeetha *et al.* 2015), (Ahamad *et al.* 2010), (Singh *et al.* 2010), (Shukla *et al.* 2010), (Golestani *et al.* 2014), (Thirumoolan *et al.* 2014), (Gökhan *et al.* 2011), (Eddy *et al.* 2009), (Shukla & Quraishi 2010), (K.Singh & Ebenso 2013). Previous studies attributed the inhibitive effect of drugs in aqueous solution to the adsorption process through the active centers on the metallic surface, which is physi- or chemi-sorption type or both together. The adsorption of the drugs molecules alters the corrosion resisting property of the tested material (Hoseinpoor & Davoodi 2015), (Singh & Quraishi 2010), (Singh *et al.* 2011). The adsorption process depends on many factors among of which are the nature and the type of charge on the metallic surface, the type of corrosive solution, the structure of the added inhibitor and the nature of its interaction with the metallic surface, (Sahin *et al.* 2002).

The aim of the present study is to discuss the inhibitive effect of famotidine as a non-toxic inhibitor towards the corrosion of C-steel in 0.5 M H<sub>2</sub>SO<sub>4</sub>. Chemical and electrochemical techniques, such as weight loss, hydrogen gas evolution, potentiodynamic polarization and EFM modulation techniques, as well as, SEM investigation are used. The adsorption mechanism and the inhibition efficiency of FA are investigated and discussed.

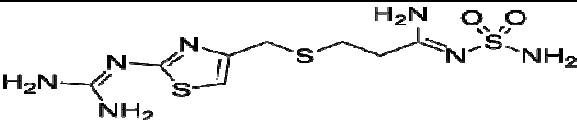
## 2. Experimental.

### 2.1. Materials

C-steel specimens having the following composition (wt.%): 0.12% C, 0.5% Mn, 0.17% Si, 0.06% S, 0.046% P and balance with iron has been used for chemical and electrochemical measurements. Steel coupons with dimensions of 2.0 cm x 7.6 cm x 1.2 cm were used for weight loss, hydrogen evolution measurements and SEM investigation. For electrochemical methods, cylindrical C-steel rods coated with Araldite except its bottom surface with surface area of 0.42 cm<sup>2</sup> are used. Prior to each run, the sample was abraded with 280, 400, 600, 800 and 1200 grades of emery papers. The specimens were washed thoroughly with bi-distilled water, ethanol, bi-distilled water, respectively, and finally dried using a filter paper before immersion in the test solution. For each run, a freshly abraded electrode was used.

Famotidine, FA, is a commercial name of 3-[(2-[(diaminomethylidene)amino]-1,3-thiazol-4-yl)methyl]sulfanyl)-N'-sulfamoylpropani –midamide is used as a corrosion inhibitor. The structure of Famotidine is shown in Table 1. Famotidine was purchased from Aldrich Chemical Co. The corrosive solution (0.5 M H<sub>2</sub>SO<sub>4</sub>) was prepared by appropriate dilution of analytical grade H<sub>2</sub>SO<sub>4</sub> using bi-distilled water.

**Table 1.** Molecular structure, molecular formula (M.F.) and molecular weight (M.W.) of Famotidine (FA).

Molecular structure	M.F.	M.W.
	C <sub>8</sub> H <sub>15</sub> O <sub>2</sub> N <sub>7</sub>	337.4

### 2.2. Weight loss method

Clean steel coupons were allowed to stand for the desired time in a closed beaker containing 100 ml 0.5 M H<sub>2</sub>SO<sub>4</sub> solution devoid of and containing different concentrations of FA. Experiments were carried out in duplicate and the mean weight losses values were reported. The procedure of weight loss study was similar to that reported before (Abd El Haleem *et al.* 2013), (Abd El Aal *et al.* 2013), (Abd El Wanees *et al.* 2016). The experimental data of mass loss can be used to determine the corrosion rate (*r*) using the equation:

$$r = \left( \frac{W_o - W_i}{St} \right) \quad (1)$$

where *W<sub>o</sub>* and *W<sub>i</sub>* are the mass loss in 0.5 M H<sub>2</sub>SO<sub>4</sub> without and with inhibitor, respectively, *S* is the total area in cm<sup>2</sup> and *t* is the immersion time, in min.

### 2.3. Hydrogen evolution method

The procedure of H<sub>2</sub> measurements was similar to that reported before (Abd El Haleem *et al.* 2013), A 100 ml of the corrosive or the inhibitive solution was introduced into the reaction vessel, containing C- steel coupon. The volume of the evolved of hydrogen gas was followed at different times.

### 2.4. Electrochemical measurements

A conventional three electrode electrochemical cell system is used for electrochemical experiment. A Pt wire was used as an auxiliary electrode. The reference electrode was SCE, while C-steel electrode was the working electrode. Before each run, the working electrode was abraded and prepared as used before, (Sangeetha *et al.* 2015), (Abd El Wanees *et al.* 2016), (Abdallah *et al.* 2016). Before starting polarization, the prepared electrode was left in the test solution until *E<sub>st</sub>* is reached. All electrochemical measurements were performed using Gamry instrument PCI300/4 Potentiostat/Galvanostat/Zra analyzer, DC105 corrosion software, EIS300 electrochemical impedance spectroscopy software, EFM140 electrochemical frequency modulation software and Echem Analyst 5.5 for data plotting, graphing, data fitting and calculating.

The potentiodynamic polarization measurements were obtained by changing the electrode potential automatically from -1000 to 150 mV vs SCE at a scan rate of 0.2 mVs<sup>-1</sup>, at 30 °C.

The surface coverage ( $\theta$ ) and inhibition efficiencies ( $\eta$  %) at different FA concentrations, are calculated using the following equations, (Abd El Wanees *et al.* 2016). “

$$\theta = \left( 1 - \frac{I_{inh}}{I_{free}} \right) \quad (2)$$

$$\eta\% = \left( 1 - \frac{I_{inh}}{I_{free}} \right) 100 \quad (3)$$

where  $I_{inh}$  and  $I_{free}$  are the corrosion current densities in 0.5M H<sub>2</sub>SO<sub>4</sub> with and without FA inhibitor, respectively.

### 2.5. Electrochemical impedance spectroscopy (EIS)

Impedance measurements were carried out in frequency range from 20 kHz to 0.5 Hz with amplitude of 5 mV peak-to-peak using AC signals at open circuit potential. The experimental impedance were analyzed and interpreted based on the equivalent circuit model (Sangeetha *et al.* 2015).

### 2.6. Scanning electronic microscope (SEM)

Two of C-steel specimens were abraded with emery papers then washed with bi-distilled water and acetone. After immersion for a period of 1 hr in 0.5 M H<sub>2</sub>SO<sub>4</sub> without and with  $1 \times 10^{-3}$  M FA, at 30°C, the C-steel specimens were pack up, cleaned with distilled water, dried using a cold air blaster for investigation under SEM using A Jeol JSM-5400 instrument.

## 3. Results and discussion

### 3.1. Weight loss measurements:

The corrosion behavior of a metal in an aqueous environment is generally characterized by the extent to which it dissolves in the solution. Fig 1 depicts the data of weight loss-time curves of the examined C-steel in aqueous solution of 0.5 M H<sub>2</sub>SO<sub>4</sub> devoid of- and containing different concentrations of famotidine, FA, at 30°C. It is clear that, the weight loss of C-steel coupons in the corrosive and the inhibitive solution increase directly with time. The loss in weight in presence of inhibitor is much lower than that obtained in free acid solution. The loss in weight becomes more lower as FA concentration is increased. In additions, the linear fitting of weight loss-time relation confirms that the dissolution of C-steel in the corrosive solution is accompanied by the formation of soluble corrosion products (Abd El Wanees *et al.* 2016), (Abdallah *et al.* 2016).

Mathematical equations based on the previous literature can be used to express the experimental data of mass loss by some of corrosion parameters such as, corrosion rate ( $r$ ), surface coverage ( $\theta$ ) and inhibition efficiencies ( $\eta$  %), as following (Abd El Haleem *et al.* 2013), (Abd El Aal *et al.* 2013), (Abd El Wanees *et al.* 2016).

$$\theta = \left( 1 - \frac{r_{inh}}{r_{free}} \right) \quad (4)$$

$$\eta\% = \left( 1 - \frac{r_{inh}}{r_{free}} \right) 100 \quad (5)$$

where  $r_{free}$  and  $r_{inh}$  are the corrosion rates calculated in 0.5 M H<sub>2</sub>SO<sub>4</sub> without and with FA inhibitor, respectively. The values of corrosion characteristic,  $r$ ,  $\theta$  and  $\eta$  % are listed in Table 2. It is clear that FA inhibitor retards the dissolution of C-steel in 0.5 M H<sub>2</sub>SO<sub>4</sub>, by decreasing the corrosion rate, which become more lower by increasing inhibitor concentration. The inhibition efficiency,  $\eta$  % is increased to take maximum value (89.5%) with  $6 \times 10^{-6}$  M FA.

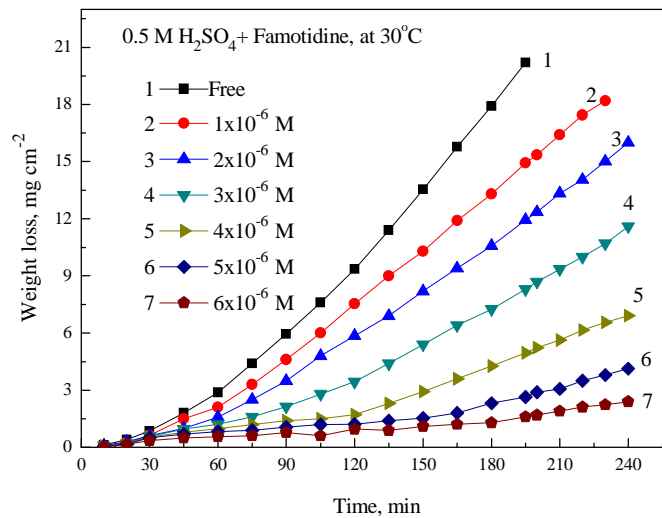


**Fig.1.** Weight loss-time curves for C- steel in 0.5M H<sub>2</sub>SO<sub>4</sub> with different concentrations of FA, at 30°C.

Fig 2A depicts the variation of rate of corrosion,  $r$ , of C-steel with the log FA concentration. S-shaped curve is obtained, confirming that the inhibition effect of FA is based on the adsorption process (Abd El Haleem *et al.* 2013), (Abd El Aal *et al.* 2013), (Abd El Wanees *et al.* 2016). The inhibitive performance of FA is suggested to be due to the adsorption of FA molecules on steel surface through the lone pair of free electrons located on N, O and S atoms, as well,  $\pi$ - electrons of double bonds (Daoud *et al.* 2015).

### 3.2. Hydrogen evolution

C-steel coupons were performed in 0.5 M H<sub>2</sub>SO<sub>4</sub> devoid of- and containing different concentrations of FA, at 30°C. The concentration of the inhibitor is varied between  $1 \times 10^{-6}$  and  $6 \times 10^{-6}$  M. Generally, there is an induction period before increasing in the volume of the evolved H<sub>2</sub> gas. This period is known before as incubation period, which is required to remove any pre-immersion oxide film on the metal surface and start metal dissolution (Abd El Haleem *et al.* 2013), (Abd El Aal *et al.* 2013), (Abd El Wanees *et al.* 2016). After incubation period, the volume of the evolved H<sub>2</sub> gas increases linearly with time due to the possible anodic dissolution of the bare metal according to the reaction:

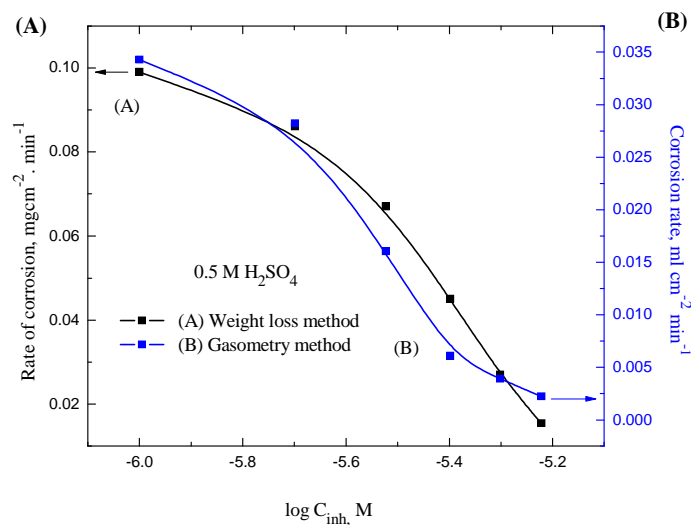


**Fig.2.** Variation of the rate of corrosion of C-steel in 0.5 M H<sub>2</sub>SO<sub>4</sub> with the logarithm of concentrations of FA, at 30°C, (A) weight loss method and (B) gasometry method.



The accompanied cathodic reaction consumes the electrons released is the overall H<sub>2</sub> reaction:



However, it the rate of corrosion is determined from slope of the linear relation between the volume, *V*, of H<sub>2</sub> evolved in ml/cm<sup>2</sup>, and the immersion time, *t*. The decrease in the rate of corrosion in presence of FA gives a sigmoidal S-shaped curve, Fig 2B. This behavior gives as an indication that the inhibition of C-steel corrosion by FA is suggested to depend on the adsorption of the inhibitive molecules on the metallic surface (Abd El Haleem *et al.* 2013), (Abd El Wanees *et al.* 2016). The values of the surface coverage ( $\theta$ ) and inhibition efficiencies ( $\eta$  %) at different concentrations of FA, are calculated from the values of corrosion rate (*r*) as usual (Abd El Haleem *et al.* 2013), (Abd El Aal *et al.* 2013), (Abd El Wanees *et al.* 2016), Table 2. It is clear that the values of  $\theta$  and  $\eta$  % takes higher values as the FA concentration is increased, due to the increase in the amount of the adsorbed FA molecules on steel surface.

**Table 2.** The calculated values of corrosion rate, *r*,  $\theta$  and  $\eta$  % for FA towards the corrosion of C-steel in 0.5 M H<sub>2</sub>SO<sub>4</sub>, at 30°C.

FA concentration, M	Mass loss method			Hydrogen evolution method		
	<i>r</i> , $\mu\text{g cm}^{-2} \text{min}^{-1}$	$\theta$	$\eta$ %	<i>r</i> , $\text{ml cm}^{-2} \text{min}^{-1}$	$\theta$	$\eta$ %
Free	146.5	--	--	0.060	--	--
1x10 <sup>-6</sup> M	99.0	0.324	32.4	0.0478	0.203	20.3
2x10 <sup>-6</sup> M	86.0	0.413	41.3	0.0384	0.360	36.0
3x10 <sup>-6</sup> M	67.0	0.543	54.3	0.0285	0.525	52.5
4x10 <sup>-6</sup> M	45.0	0.693	69.3	0.0199	0.668	66.8
5x10 <sup>-6</sup> M	27.0	0.816	81.6	0.0132	0.780	78.0
6x10 <sup>-6</sup> M	15.4	0.895	89.5	0.0055	0.908	90.8

### 3.3. Potentiodynamic polarization measurements

The curves of the potentiodynamic polarization curves for C-steel in 0.5M H<sub>2</sub>SO<sub>4</sub> without and with additions of various concentrations of FA inhibitor are discussed. Both the cathodic and anodic polarization curves in presence of FA inhibitor are suppressed, as due to the increase in the overvoltage of each of cathodic and anodic processes This behavior could prove that the mechanism of hydrogen evolution reaction is activation-controlled process, and both the hydrogen evolution and the anodic dissolution mechanisms are not altered (Abdallah *et al.* 2016), (Fekry & Ameer 2011). The anodic and cathodic Tafel slopes take little change in presence of FA suggesting that the adsorption of FA molecules on the anodic and cathodic sites is controlled by a mixed-type, by blocking of both the anodic and cathodic reaction sites, (Abdallah *et al.* 2016), (Fekry & Ameer 2011), (Fouda *et al.* 2016). The  $\eta$  % obtained from potentiodynamic polarization measurements are increased with increasing FA concentrations, to reach 77% and 90 % with 4x10<sup>-6</sup> M and 6x10<sup>-6</sup> M, successively. The obtained values are close to that deduced from weight loss and gasometry measurements.

### 3.4. Electrochemical impedance spectroscopy (EIS)

The inhibition performance of an inhibitor on a metallic surface depends on many factors among of which is the chemical structure of the inhibitor, the nature of the metal, and also on the experimental conditions such as the immersion time, pH of the solution, as well as, the concentration of the adsorbent (Kerte & Hammouti 1996), (Li *et al.* 2009). The effect of FA on the corrosion of C-steel in H<sub>2</sub>SO<sub>4</sub> was also studied by EIS method to confirm the results obtained by other used methods. The curves of Fig.3 depicts the Nyquist plots for C-steel in 0.5 M H<sub>2</sub>SO<sub>4</sub> solution in presence of different concentrations FA inhibitor, at 30°C. The existence of the single semicircle proves the single charge transfer process accompanying the metallic dissolution step, which is uninfluenced by the presence FA. The presence of non-perfect of semicircles in Fig 3, could be interpreted to the frequency dispersion effect as due to electrode roughness and inhomogeneity effect (Shalabi *et al.* 2014), (Lebrini *et al.* 2007). To analyze the impedance spectra, the equivalent circuit given in Fig 4 is used. In this circuit, *R<sub>s</sub>* refers to the solution resistance between the steel electrode and the reference electrode while *R<sub>ct</sub>* represents charge-transfer resistance and *C<sub>dl</sub>* represents the electrochemical double layer capacitance. Generally, the presence of inhibitor enhances *R<sub>ct</sub>* and decreases *C<sub>dl</sub>*. The lowering in *C<sub>dl</sub>* values in presence of inhibitor can be suggested to the presence of a protective film formed as due to adsorption of the inhibitor on metal surface (Abd El Wanees *et al.* 2016), (Shalabi *et al.* 2014), (Lebrini *et al.* 2007), (Obot *et al.* 2009), (Hui *et al.* 2011).

The values of the charge transfer resistance,  $R_{ct}$ , are calculated for different concentrations of FA, from the difference in impedance values at lower and higher frequencies using the equation (Hong & Jepsen 2001).

$$R_{ct} = [Z_{real} \text{ (at low frequency)} - Z_{img} \text{ (at high frequency)}] \quad (8)$$

The values of the  $C_{dl}$  obtained from the analysis of Nyquist diagram at the maximum frequency  $f_{max}$ , at the maximum imaginary impedance  $Z_{max}$  and the resistance of charge transfer  $R_{ct}$  (diameter of high frequency loop) using the equation (Yadav *et al.* 2004).

$$C_{dl} = \left( \frac{1}{2\pi f_{max} R_{ct}} \right) \quad (9)$$

The values of surface coverage ( $\theta$ ) and the percentage inhibition efficiency ( $\eta'$  %), are calculated from the data of  $R_{ct}$  values using the equations (10) and (11) (Khaled 2006) :

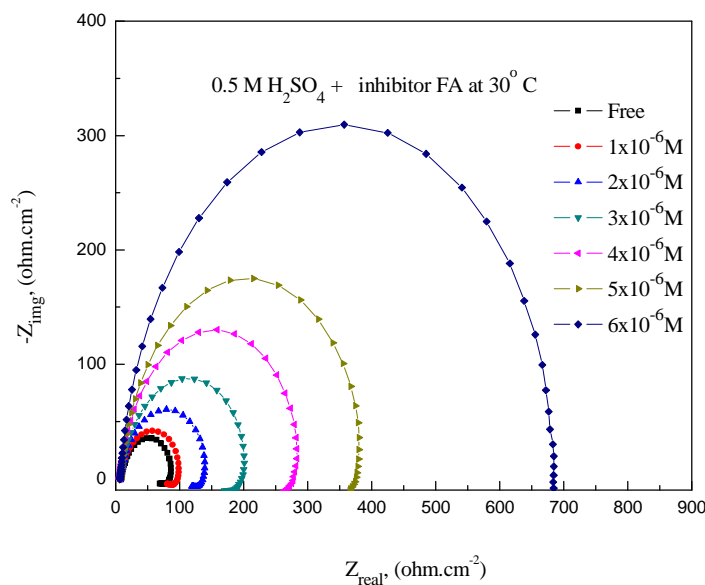


**Fig 3:** Nyquist plots for corrosion of C-steel in 0.5 M  $H_2SO_4$  in the absence and presence of different concentrations of FA, at 30°C.

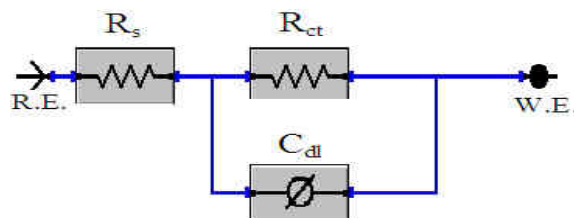


**Fig 4.** Equivalent circuit compatible with the experimental impedance data.

$$\theta = \left( 1 - \frac{R_{ct,inh} - R_{ct}}{R_{ct,inh}} \right) \quad (10)$$

$$\eta\% = \left( 1 - \frac{R_{ct,inh} - R_{ct}}{R_{ct,inh}} \right) 100 \quad (11)$$

where  $R_{ct, inh}$  and  $R_{ct}$  are the charge transfer resistance values calculated with and without FA inhibitor, respectively, in 0.5 M  $H_2SO_4$ . The calculated data of the electrochemical parameters of EIS measurements are tabulated in Table 4. It is obvious, from the data of this table, the increase in the charge transfer resistance,  $R_{ct}$  and the decrease in the double layer capacitance,  $C_{dl}$ , with increasing FA concentration. This behavior proves that the inhibition of C-steel corrosion in  $H_2SO_4$  solution by the action of FA inhibitor can be related to the adsorption process, forming a protective layer on metal surface (Hong & Jepsen 2001). In addition, the values of inhibition efficiency ( $\eta'$  %) in presence of FA takes higher values with increasing inhibitor concentration to reach 80.85% with  $1 \times 10^{-3}$  M FA.

**Table 4.** EIS data of C-steel in 0.5 M  $H_2SO_4$  at different concentrations of FA, at 30° C.

Solution, M	$C_{dl} \times 10^{-5}$ , F	$R_{ct}$ , $\Omega$	$\theta$	$\eta$ %
Free	2.86	71.29	--	--
$1 \times 10^{-6}$ M	2.59	99.00	0.28	28
$2 \times 10^{-6}$ M	2.60	124.5	0.43	43
$3 \times 10^{-6}$ M	2.70	187.1	0.62	62
$4 \times 10^{-6}$ M	2.01	272.1	0.74	74
$5 \times 10^{-6}$ M	1.85	373.5	0.81	81
$6 \times 10^{-6}$ M	1.44	684.9	0.90	90

The impedance values in presence of inhibitor, FA are larger than in blank solution and increase with increasing inhibitor concentration. The values of  $\eta'$  % obtained from impedance measurements are consistent with that obtained with other experimental techniques.

### 3.5. Electrochemical Frequency Modulation measurements

EFM spectra are shown in Fig 5 (A&B) for C-steel in 0.5 M  $H_2SO_4$  without and with  $5 \times 10^{-6}$  M FA, respectively. Similar curves are obtained in other concentrations. EFM spectra show non-linear response. Non-linear response contains enough information about the corroding system, so that the corrosion current can be calculated directly. The larger peaks were used to calculate the corrosion current density ( $i_{corr}$ ), slopes ( $\beta_a$  and  $\beta_c$ ) and the causality factors (CF-2 and CF-3) (Fouda *et al.* 2014). These electrochemical corrosion kinetic parameters at different concentrations of FA in 0.5 M  $H_2SO_4$ , at 30°C, were listed in Table 5. The inhibition efficiency,  $\eta_{EFM}$  %, calculated from equation (12), increases by increasing the FA concentration.

$$\eta_{EFM} \% = \left( 1 - \frac{i_{corr}}{i_{corr}^{\circ}} \right) 100 \quad (12)$$

where  $i_{corr}^{\circ}$  and  $i_{corr}$  are corrosion current densities in 0.5 M  $H_2SO_4$  devoid of and containing FA, successively. The causality factors CF-2 and CF-3, Table 5, are close to their theoretical values of 2.0 and 3.0, respectively, indicating that the measured data are reliable (Fouda *et al.* 2014), (Bosch *et al.* 2001). The calculated inhibition efficiencies obtained from EFM measurements are in good agreement with that obtained from other measurements.

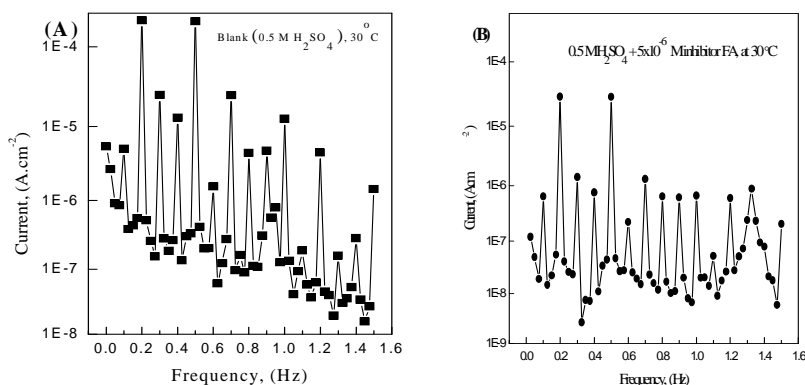


**Fig 5.** EFM spectra for C-steel in 0.5 M H<sub>2</sub>SO<sub>4</sub> (A) devoid of and (B) containing 5x10<sup>-6</sup> M FA.

**Table 5.** Electrochemical kinetic parameters obtained from EFM technique for the corrosion of C-steel in 0.5 M H<sub>2</sub>SO<sub>4</sub> at different concentrations of FA, at 30°C.

Solution	$i_{corr}$ , $\mu A$	$\beta_a$ , $V dec^{-1} \times 10^{-3}$	$\beta_c$ , $V dec^{-1} \times 10^{-3}$	CF-2	CF-3	$\theta$	IE %
Free	273.3	65.49	131.5	1.985	3.167		
1x10 <sup>-6</sup> M	194.8	60.73	134.2	1.966	2.970	0.29	29
2x10 <sup>-6</sup> M	147.7	56.60	130.5	1.971	3.667	0.46	46
3x10 <sup>-6</sup> M	95.25	51.50	119.6	1.935	2.917	0.65	65
4x10 <sup>-6</sup> M	61.54	52.50	104.7	1.930	2.833	0.77	77
5x10 <sup>-6</sup> M	43.90	54.44	97.61	2.042	2.769	0.84	84
6x10 <sup>-6</sup> M	22.81	62.74	88.41	1.907	2.964	0.92	92

### 3.6. Scanning electron micrographs (SEM):

Scanning electron micrographs for C-steel samples after immersion for a period of 1 hr in the corrosive solution in the absence and presence of 5x10<sup>-6</sup> M FA are investigated. Fig 6(A&B) represented micrographs for C-steel after immersion in (A) 0.5 M H<sub>2</sub>SO<sub>4</sub> and (B) 0.5 M H<sub>2</sub>SO<sub>4</sub> + 5 x10<sup>-6</sup> M FA. Investigation of the SEM micrographs taken in 0.5 M H<sub>2</sub>SO<sub>4</sub> solution in absence of inhibitor, Fig 6A, explores that the surface C-steel sample was strongly attacked surrounded by corrosion products. In presence of FA inhibitor, Fig 6B, shows that the surface of C-steel becomes coated by cracked cover layer, compared with that of free acid (Khamis *et al.* 2013). This proves that the FA inhibitor is adsorbed on metal surface forming a thick protective layer, hindering the corrosion process (Rudresh & Mayanna 1977).

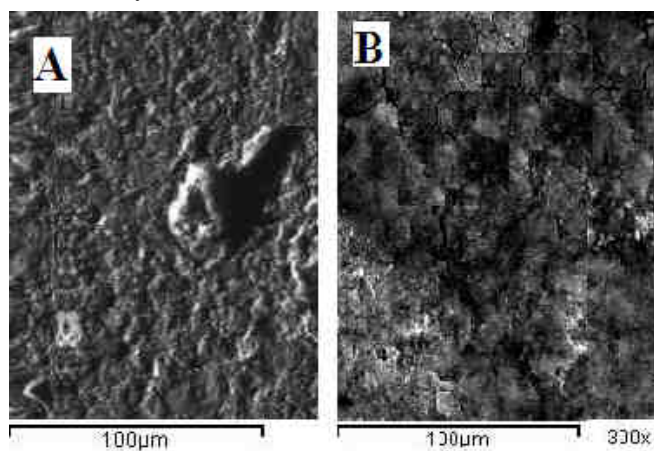


**Fig 6.** SEM for C-steel after immersion for a period of 30 min in (A) 0.5 M H<sub>2</sub>SO<sub>4</sub> and (B) 0.5 M H<sub>2</sub>SO<sub>4</sub> + 5x 10<sup>-6</sup> M FA, respectively, at 30°C.



### 3.6. Effect of temperature

The effect of temperature on the rate of corrosion of C-steel in solutions of 0.5 M H<sub>2</sub>SO<sub>4</sub> devoid of- and containing different concentrations FA (1x10<sup>-6</sup> to 6 x10<sup>-6</sup>M) is studied by hydrogen evolution method. The data revealed that increasing the temperature increases the rate of corrosion of C-steel surfaces both in the absence and presence of FA. On the other hand, the corrosion rate decreases as the inhibitor concentration is increased. The inhibition efficiency decreases with temperature although it increases with increase the inhibitor concentration, Table 6. When the temperature is increased, surface coverage is reduced as due to the desorption of FA molecules from the C-steel surface (Ebenso & Obot 2010). The decrease in the rate of adsorption of FA at higher temperature, could be attributed to the performance of physical adsorption type on steel surface (Maayta & Rawashdeh 2004), (Abboud *et al.* 2009).

The dependence of the rate of corrosion on temperature can be expressed by Arrhenius and transition state equations (Abd El Aal *et al.* 2013), (Abd El Wanees *et al.* 2016), (Abdallah *et al.* 2016).

$$\log r = \frac{-\Delta E_a}{2.303RT} + \log A \quad (13)$$

$$r = \frac{RT}{Nh} \exp\left(\frac{\Delta S_a}{R}\right) \exp\left(\frac{-\Delta H_a}{RT}\right) \quad (14)$$

where  $r$  is the corrosion rate,  $\Delta E_a$  is the apparent activation energy,  $T$  is the absolute temperature,  $A$  is a frequency factor,  $\Delta H_a$  is the apparent enthalpy of activation,  $\Delta S_a$  is the apparent entropy of activation,  $h$  is Planck's constant and  $N$  is the Avogadro's number, respectively.

The values of  $\log r$  ( $\mu\text{g cm}^{-2} \text{min}^{-1}$ ), obtained at different temperatures, confirm linear relation with  $1/T$ , Fig 7. The activation energies values,  $\Delta E_a$  were calculated from the slope of the plots of Fig 7 and are given in Table 7. The value of  $\Delta E_a$  for blank was 64.14 kJ/mol and takes higher values in presence of FA, 71.61 kJ/mol to 177.11 kJ/mol. This is considering as an indication of a strong inhibitive action of FA, as due to the increase in the energy barrier of the corrosion process, emphasizing the physisorption process (Guan *et al.* 2004). The higher values of  $\Delta E_a$  in presence of FA compared to the blank, support physical adsorption mechanism (Mobin *et al.* 2016).

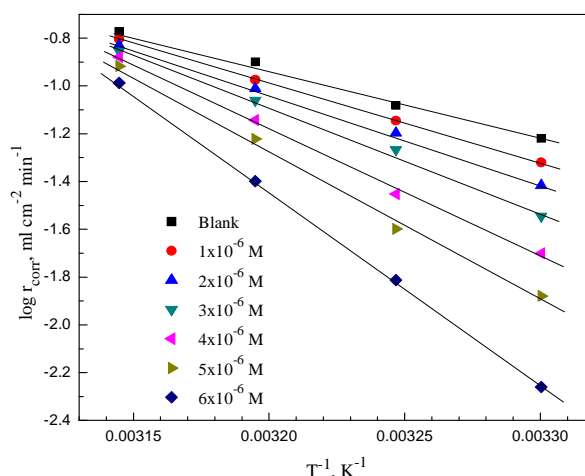


**Fig 7.** Arrhenius plots for C-steel in 0.5M H<sub>2</sub>SO<sub>4</sub> devoid of and containing different concentrations of FA.

Plotting of  $\log (r/T)$  against  $1/T$  (Eq. 14) for C-steel dissolution in 0.5 M H<sub>2</sub>SO<sub>4</sub> devoid of- and containing different concentrations FA, gave straight lines as shown in Fig 8. Values of  $\Delta H_a$  and  $\Delta S_a$  were calculated and tabulated in Table 7. The positive sign of  $\Delta H_a$  reflects the endothermic nature of metal corrosion in H<sub>2</sub>SO<sub>4</sub> solution. In addition, the increase in  $\Delta S_a$  values with increasing inhibitor concentration reveals increase in

disordering on going from reactants to the activated complex (Benadellah *et al.* 2006). This behavior can be explained as a result of a substitution process between H<sub>2</sub>O and FA molecules on C-steel surface (Dahmani *et al.* 2010).

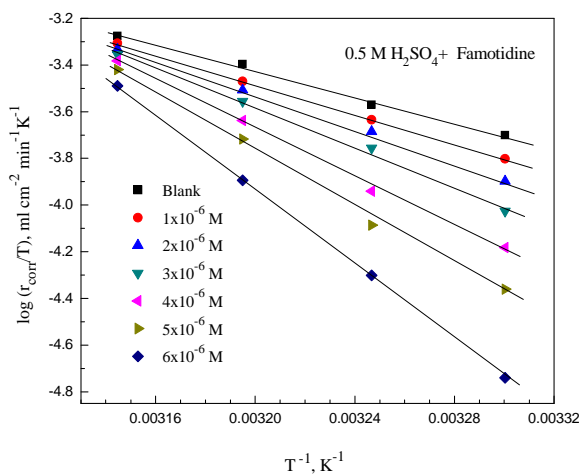


**Fig 8.** Transition-state plots for C-steel in 0.5M H<sub>2</sub>SO<sub>4</sub> devoid of and containing different additions of FA.

**Table 6.** The values of corrosion rate,  $r$ ,  $\theta$  and  $\eta$  % for different concentrations of FA towards the corrosion of C-

FA, M	303K			308 K			313K			318K		
	$r$ , ml/cm <sup>2</sup> min <sup>-1</sup>	$\theta$	$\eta$ %	$r$ , ml/cm <sup>2</sup> min	$\theta$	$\eta$ %	$r$ , ml/cm <sup>2</sup> min	$\theta$	$\eta$ %	$r$ , ml/cm <sup>2</sup> min	$\theta$	$\eta$ %
Free	0.060	--	--	0.083	--	--	0.126	--	--	0.169	--	--
1x10 <sup>-6</sup> M	0.0478	0.203	20.3	0.070	0.156	15.6	0.110	0.127	12.7	0.157	0.071	7.1
2x10 <sup>-6</sup> M	0.0384	0.360	36.0	0.068	0.214	21.4	0.097	0.23	23.0	0.148	0.124	12.4
3x10 <sup>-6</sup> M	0.0285	0.525	52.5	0.050	0.398	39.8	0.087	0.31	31.0	0.140	0.172	17.2
4x10 <sup>-6</sup> M	0.0199	0.668	66.8	0.035	0.578	57.8	0.072	0.429	42.9	0.132	0.219	21.9
5x10 <sup>-6</sup> M	0.0132	0.780	78.0	0.025	0.699	69.9	0.062	0.508	50.8	0.121	0.284	28.4
5x10 <sup>-6</sup> M	0.0055	0.908	90.8	0.015	0.819	81.9	0.043	0.659	65.9	0.110	0.349	34.9

steel in 0.5 M H<sub>2</sub>SO<sub>4</sub>, at 30°C.

**Table 7:** Thermodynamic parameters,  $\Delta E_a$ ,  $\Delta H_a$ ,  $\Delta S_a$  for C-steel in 0.5M H<sub>2</sub>SO<sub>4</sub> in the absence and presence of different concentrations of FA.

Solution	$\Delta E_a$ , kJ mol <sup>-1</sup>	$\Delta S_a$ , J mol <sup>-1</sup> K <sup>-1</sup>	$\Delta H_a$ , kJ mol <sup>-1</sup>
Free	64.14	-67.93	61.46
1 x10 <sup>-6</sup> M	71.61	-45.34	68.93
2 x10 <sup>-6</sup> M	79.08	-21.98	76.59
3 x10 <sup>-6</sup> M	103.97	55.76	101.48
4 x10 <sup>-6</sup> M	147.43	191.7	144.94
5 x10 <sup>-6</sup> M	158.35	223.68	155.67
6 x10 <sup>-6</sup> M	177.11	279.78	174.43

### 3.7. Adsorption isotherm

The values of surface coverage ( $\theta$ ) calculated by hydrogen evolution methods for different concentrations of FA are used to test the suitable type of adsorption isotherms. Different types of isotherms, such as, Temkin, Langmuir, Frumkin, Frundlich, Bockris-Swinkels and Flory-Huggins isotherms, are used to get the best fit isotherm. Based on the value of correlation coefficient,  $R^2$ , the best fit isotherm was found to obey Freundlich type. This type of isotherm can be represented by the mathematical equation (Kliskic *et al.* 2000):

$$\theta = K_{ads} C^n \quad (15)$$

or

$$\log \theta = \log K_{ads} + n \log C \quad (16)$$

where  $0 < n < 1$ ,  $\theta$  is the surface coverage,  $K_{ads}$  is the adsorption equilibrium constant of the adsorption process.

Plotting of  $\log \theta$  versus  $\log C$ , at different temperatures, gives straight-line relation, Fig 9, confirming Frundlich adsorption isotherm. The corresponding linear regression parameters are listed in Table 8. Each of the linear correlation coefficient and slope are approximately equal to one, suggesting that the adsorption of FA on C-steel surface obeys Frundlich adsorption isotherm. This behavior suggest that the inhibition effect is resulted from adsorption of inhibitor molecules on steel surface forming an insulating film that isolate the metal from the corrosive solution. In addition, the values of the adsorption constant,  $K_{ads}$ , can be calculated from the value of the intercept, according to equation 16. The large values of  $K_{ads}$  are an indication of strong adsorption of FA on C-steel surface. It is noteworthy to see that, the value of  $K_{ads}$  is decreased as the temperature is increased (Table 8) suggest that there is rearrangement and detachment of inhibitor molecules from electrode surface due to desorption process.

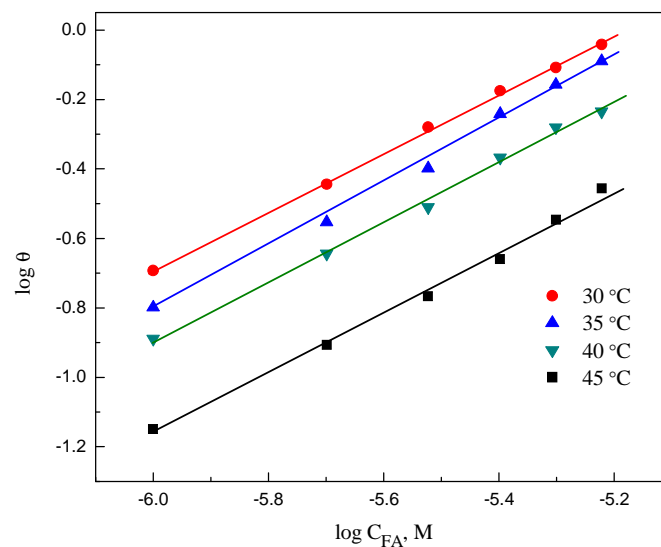


**Fig 9.** Frundlich adsorption isotherm of FA on steel surface, at different temperatures.

The standard free energy of adsorption,  $\Delta G^\circ$ , can be calculated from the value of the adsorption constant,  $K_{ads}$ , according to the equation (Abd El Haleem *et al.* 2014):

$$K_{ads} = \frac{1}{55.5} \exp\left(\frac{-\Delta G^\circ}{RT}\right) \quad (17)$$

where  $T$  is the absolute temperature, 55.5 is the concentration of water expressed in molar value and  $R$  is the gas constant equal to  $8.314 \text{ Jk}^{-1} \text{ mol}^{-1}$ . The calculated values of  $K_{ads}$  and  $\Delta G^\circ$  are tabulated in Table 8. The negative

value of  $\Delta G^\circ$  gives an indication that the adsorption of FA on C-steel surface is a spontaneous process. As is already well established, values of  $\Delta G^\circ_{ads}$  up to  $-20$  kJ/mol are associated with electrostatic interaction between the charged inhibitor molecules and the charged metal surface (physi-sorption). On the other hand, values of  $\Delta G^\circ_{ads}$ , which are more negative than  $-40$  kJ/mol involve sharing or transfer of electrons from the organic inhibiting species to the metal surface to form a metal bond, chemisorption (Solomon *et al.* 2010), (Gürten *et al.* 2007). In our case, the calculated  $\Delta G^\circ_{ads}$  values are,  $-34.82$ ,  $-34.30$ ,  $-33.85$  and  $-33.28$  kJ/mol at 30, 35, 40 and 45 °C, successively. These values are between the two stated threshold values suggested that there is an electrostatic interaction between the charged inhibitor molecules and the charged metal surface (physi-sorption type) beside the chemisorption, mixed mechanism.

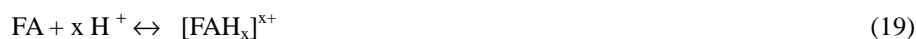
$$K_{ads} = \frac{1}{55.5} \exp\left(\frac{-\Delta G}{RT}\right) \quad (18)$$

**Table 8:** Correlation coefficient  $R^2$ , adsorption equilibrium constant,  $K_{ads}$  and free energy of adsorption  $\Delta G^\circ_{ads}$  of FA on C-steel in 0.5M  $H_2SO_4$ , at different temperatures.

Temperature	$R^2$	$K_{ads}, M^{-1}$	$\Delta G^\circ_{ads}, KJ mol^{-1}$
303	99.88	63622	-37.99
305	99.99	129315	-40.78
308	99.78	171100	-41.77
313	99.89	178090	-42.52

### 3.8. Inhibition mechanism:

The inhibitive effect of famotidine, FA, towards the corrosion of C-steel in 0.5 M  $H_2SO_4$  can be discussed through a number of variable factors among of which are the presence of adsorption centers, suitable bulky molecular size and mode of interaction with the metal surface (Singh & Quraishi 2012), (Singh & Quraishi 2011). Physisorption requires the presence of both electrically charged metallic surface and bulky charged inhibitive species having heteroatoms rich with lone pair of electrons. However, the used inhibitor is an organic base comprises seven nitrogen atoms, which can easily protonated in an acidic medium, to be bulky charged molecule. The resulted famotidine cations, can be represented by  $[FAH_x]^{x+}$ , become in equilibrium with the corresponding molecular form, FA, according to equation (19).



The protonated famotidine cations,  $[FAH_x]^{x+}$ , however, could be attached to the C-steel surface by means of electrostatic interaction between  $SO_4^{2-}$  and protonated famotidine since the C-steel surface has positive charge in  $H_2SO_4$  medium (Singh *et al.* 2011). This could further be explained based on the assumption that in the presence of  $SO_4^{2-}$ , the negatively charged  $SO_4^{2-}$  would attach to positively charged surface. When famotidine adsorbs on the C-steel surface, electrostatic interaction takes place by partial transference of electrons from the polar atoms (N, S and O atoms) of famotidine to the metal surface. However, the decrease in inhibition efficiencies at higher temperatures can be attributed to the desorption process from metallic surface (Xianghong *et al.* 2008).

## 5. Conclusion

The corrosion rate of C-steel in 0.5 M  $H_2SO_4$  in presence of different concentrations of famotidine is examined by different chemical and electrochemical techniques. The study indicated that:

1. Famotidine acts as a mixed-type inhibitor for corrosion C-steel in  $H_2SO_4$ .
2. Inhibition efficiency increases as the concentration of famotidine is increased.
3. The adsorption of famotidine on C-steel surface follows Frundlich adsorption isotherm.
4. The increase in  $\Delta E_a$  values in presence of higher concentration of famotidine is related to the higher adsorption effect of the inhibitor on the metallic surface.
5. The values of  $\Delta G^\circ_{ads}$  varied between  $-37.99$  and  $-42.52$ kJ/mol, at the examined temperatures range explaining the spontaneous adsorption process confirming physisorption and chemisorption mechanism.

## References

- Bentiss F., Tranisnel M., Lagrence M. (2001) *J. Appl. Electrochem.*, 31,41-48.
- Chetouani A., Medjahed K., Benabadi K. E., Hammouti B., Kertit S., Mansri A.(2003) *Prog. Org. Coat.*, 46, 312 –316.
- Ashassi-Sorkhabi H., Majidi M.R., Seyyedi K. (2004) *Appl. Surf. Sci.*, 225,176-185.
- Ashassi-Sorkhabi H., Shaabani B., Seifzadeh D.(2005) *Electrochim. Acta*, 50, 3446-3452.
- Daoud D., Douadi T., Hamani H., Chafaa S., Al-Noaimi M. (2015) *Corros. Sci.*, 84, 21–37.
- El Azzouzi M., Aouniti A., Tighadouin S., Elmsellem H., Radi S., Hammouti B., El Assyry A., Bentiss F., Zarrouk A. (2016) *J. Mol. Liq.*, 221633-641.
- Evelin Gutiérrez, José A. Rodríguez, Julián Cruz-Borbolla, José G. Alvarado-Rodríguez, Pandiyan Thangarasu (2016) *Corros. Sci.* 108, 23-35.
- Abd El-Lateef H. M., Abo-Riya M. A., Tantawy A. H. (2016) *Corros. Sci.* 108, 94-110.
- Kowsari E., Arman S.Y., Shahini M.H., Zandi H., Ehsani A., Naderi R., Pourghasemi Hanza A., Mehdipour M., (2016) *Corros. Sci.* in press.
- Pourghasemi Hanza A., Naderi R., Kowsari E., Sayebani M. (2016) *Corros. Sci.*, 107, 96–106.
- Sangeetha Y., Meenakshi S., Sairam Sundaram C. (2015) *Pigment & Resin Technology* 44, 371 – 378.
- Ahamad I., Prasad R., Quraishi M.A. (2010) *Corros. Sci.*, 52, 3033-3041.
- Singh A. K., Quraishi M.A. (2010) *Corros. Sci.*, 52, 152-160
- Shukla S. K., Quraishi M.A. (2010) *Mater. Chem. Phys.*, 120, 142-147.
- Golestani Gh., Shahidi M., Ghazanfar D. (2014) *Appl. Surf. Sci.*, 308, 347-362.
- Thirumoolan D., Vikas A. Katkar, Gunasekaran G., Tapan Kanai, Anver Basha K. ( 2014) *Progress in Organic Coatings*, 77, 1253-1263
- Gökhan Gece (2011) *Corros. Sci.* 53, 3873–3898.
- Eddy N.O., Odoemelam S.A., Ekwumemgbo P. (2009) *Sci. Res. Essays* 4, 033–038.
- Shukla S. K., Quraishi M.A. (2010) *Corros. Sci.*, 52, 314-321.
- K.Singh A., Ebenso Eno E. (2013) *Res. Chem. Intermediat.*, 39,1823-1831
- Hoseinpoor M., Davoodi A. (2015) *Res. Chem. Intermediat.*, 41, 4255–4272.
- Singh A. K., Quraishi M.A. (2011) *J. Appl. Electrochem.*, 41, 7-18.
- Singh A. K., Shukla S. K., Singh M. Quraishi M.A. (2011) *Mater. Chem. Phys.*, 129, 68-76.
- Sahin M., Bilgic S., Yilmaz H., (2002) *Appl. Surf. Sci.*, 195. 1.
- Abd El Haleem S. M., Abd El Wanees S., Abd ElAal E.E., Farouk A. (2013)*Corros. Sci.*, 68,1-13.
- Abd El Aal E. E., Abd El Wanees S., Abd El Haleem S. M., Farouk A. (2013)*Corros. Sci.*, 68, 14-24.
- Abd El Wanees S., Alahmdi M. I., Rashwan S.M., Kamel M. M., Abd Elsadek M.G. (2016) *Int. J. Electrochem. Sci.*, 11, In press.
- Abdallah M., Al-Tass H. M., Al Jahdaly B.A., Fouda A.S. (2016) *J. Mol. Liq.*, 216, 590 -597.
- Fekry A. M., Ameer M. A. *Int. J. Hydrogen Energy* (2011) 36,11207 -11215.
- Fouda A.S., Etaiw S. El-Din H., El-bendary M. M., Maher M.M. (2016) *J. Mol. Liq.*, 213, 228 –234.
- Kerte S., Hammouti B. (1996) *Appl. Surf. Sci.* 93, 59-66.
- Li X., Deng S., Fu H., Li T. (2009) *Electrochim. Acta*, 54, 4089–4098.
- Shalabi K., Abdallah Y. A., Hassan Hala M., Fouda A.S. (2014) *Int. J. Electrochem. Sci.*, 9, 1468-1487.
- Lebrini M., Lagrenee M., Vezin H., Traisnel M., Bentiss F. (2007) *Corros. Sci.*, 49, 2254-2269.
- Obot I. B., Obi-Egbedi N.O., Umoren S. A. (2009) *Corros. Sci.*, 51, 276 -282.
- Hui P.X., Min G., Xuan Z. Yu, Qin W., Rong H. B. (2011) *Sci. China, Ser. B:Chem.* 4332 –4339.
- Hong T., Jepson W. P. (2001) *Corros. Sci.*, 43, 1839-1849.

- Yadav A. P., Nishikata A., Tsuru T. (2004) *Corros. Sci.*, 46, 169 -181.
- K. F. Khaled (2006) *Appl. Surf. Sci.*, 252, 4120-4128.
- Fouda A.S. , Shalabi K., Elewady G.Y., Merayyed H.F. (2014) *Inter. J. Electrochem, Sci.*, 9,7038-7058.
- Bosch R. W., Hubrecht J., Bogaerts W. F., Syrett B. C. (2001) *Corrosion*, 57, 60-70.
- Khamis A., Saleh M. M., Awad M. I., El-Anadouli B.E. (2013) *Corros. Sci.*, 74, 83-91.
- Rudresh H. B., Mayanna S. M. (1977) *J. Environ. Sci. Technol.*, 122, 251–256.
- Ebenso E.E., Obot I.B. (2010) *Int. J. Electrochem. Sci.* 5, 2012- 2035.
- Maayta A.K., Al-Rawashdeh N.A.F. (2004) *Corros. Sci.*, 46, 1129 -1140.
- Abboud Y., Abourriche A., Saffaj T., Berrada M., Charrouf M., Bennamara A., Hannache H. (2009), *Desalination*, 237, 175-189.
- Guan N. M., Xueming L., Fei L. (2004) *Mater. Chem. Phys.*, 86, 59-68.
- Mobin M. , Zehra S., Praveen M. (2016)*J. Molecular Liq.*, 216, 598.
- Benadallah M., Aouniti A., Dafali A., Hammouti B., Benkaddaour M., A. Yahyi, A. Ettouhami, *Appl. Surf. Sci.* 252(2006)8341-8347.
- Dahmani M., El-Touhami A., Al-Deyab S.S., Hammouti B., Bouyanzer A. (2010) *Inter. J. Electrochem. Sci.* 5,1060-1069.
- Kliskic M., Radosevic J., Gudic S., Katalinic V. (2000) *J. Appli. Electrochem.*, 30, 823-830.
- Abd El Haleem S. M., Abd El Wanees S., Baghat A. (2014) *Corros. Sci.*, 87, 321-333.
- Solomon M.M., Umoren S.A., Udosoro I.I., Udoh A.P. (2010) *Corros. Sci.*, 52, 1317-1325.
- Gürten A.A., Kayakırlmaz K., Erbil M., *Constr. Build. Mater*(2007) 21, 669-676.
- Singh A. K., Quraishi M. A. (2012) *Int. J. Electrochem. Sci.*, 7, 3222-3241. ,
- Singh A. K., Quraishi M. A (2011) *J. Appl. Electrochem.* 41, 7-18.
- Singh A. K., Quraishi M. A., Ebenso E. E. (2011) *Int. J. Electrochem. Sci* 6, 5676-5688.